Composition of the Rex Chert and Associated Rocks of the Permian Phosphoria Formation: Soda Springs Area, SE Idaho

By

James R. Hein[1], Brandie McIntyre[1], Robert B. Perkins[1], David Z. Piper[1], James Evans[2]

Open-File Report 02-345

2002

Prepared in Collaboration With
U.S. Bureau of Land Management
U.S. Forest Service
Agrium U.S. Inc.
Astaris LLC
J.R. Simplot Company
Rhodia Inc.
Monsanto Co.

This report is preliminary and has not been reviewed for conformity with U.S. Geological Survey editorial standards or with the North American Stratigraphic Code. Any use of trade, firm, or product names is for descriptive purposes only and does not imply endorsement by the U.S. Government.

U. S. DEPARTMENT OF THE INTERIOR
U. S. GEOLOGICAL SURVEY

[1]U.S. Geological Survey, 345 Middlefield Rd., Menlo Park, CA, 94025
[2]U.S. Geological Survey, 904 W. Riverside Ave., Spokane, WA, 99201

CONTENTS

FIGURES

TABLES

ABSTRACT

This study, one in a series, reports bulk chemical and mineralogical compositions, as well as petrographic and outcrop descriptions of rocks collected from three measured outcrop sections of the Rex Chert member of the Phosphoria Formation in SE Idaho. The three measured sections were chosen from ten outcrops of Rex Chert that were described in the field. The Rex Chert overlies the Meade Peak Phosphatic Shale Member of the Phosphoria Formation, the source of phosphate ore in the region. Rex Chert removed as overburden comprises part of the material disposed in waste-rock piles during phosphate mining. It has been proposed that the chert be used to cap and isolate waste piles, thereby inhibiting the leaching of potentially toxic elements into the environment. It is also used to surface roads in the mining district. The rock samples studied here constitute a set of individual chert beds that are representative of each stratigraphic section sampled. The informally named cherty shale member that overlies the Rex Chert in measured section 1 was also described and sampled. The upper Meade Peak and the transition zone to the Rex Chert were described and sampled in section 7. The cherts are predominantly spicularite composed of granular and mosaic quartz, and sponge spicules, with various but minor amounts of other fossils and detrital grains. The cherty shale member and transition rocks between the Meade Peak and Rex Chert are siliceous siltstones and argillaceous cherts with ghosts of sponge spicules and somewhat more detrital grains than the chert. The overwhelmingly dominant mineral is quartz, although carbonate beds are rare in each section and are composed predominantly of calcite and dolomite in addition to quartz. Feldspar, mica, clay minerals, calcite, dolomite, and carbonate fluorapatite are minor to trace minerals in the chert.

The mean concentrations of oxides and elements in the Rex Chert and the cherty shale member are dominated by SiO_2, which averages 94.6%. Organic-carbon contents are generally very low in the chert, but are up to 1.8 wt. % in cherty shale member samples and up to 3.3% in samples from the transition between the Meade Peak and Rex Chert. Likewise, phosphate (P_2O_5) is generally low in the chert, but can be up to 3.1% in individual beds. Selenium concentrations in Rex Chert and cherty shale member samples vary from <0.2 to 138 ppm, with a mean concentration of 7.0 ppm. This mean Se content is heavily dependent on two values of 101 and 138 ppm for rocks from the transition zone between the Meade Peak and Rex Chert. Without those two samples, the mean Se concentration would be <1.0 ppm. Other elements of environmental interest, As, Cr, V, Zn, Hg, and Cd, are generally near or below their content in average continental shale. Stratigraphic changes (equivalent to temporal changes in the depositional basin) in chemical composition of rocks are notable either as uniform changes through the sections or as distinct differences in the mean composition of rocks that compose the upper and lower halves of the sections.

Q-mode factors are interpreted to represent the following rock and mineral components: chert-silica component consisting of Si (± Ba); phosphorite-phosphate component composed of P, Ca, As, Y, V, Cr, Sr, and La (± Fe, Zn, Cu, Ni, Li, Se, Nd, Hg); shale component composed of Al, Na, Zr, K, Ba, Li, and organic C (± Ti, Mg, Se, Ni, Fe, Sr, V, Mn, Zn); carbonate component (dolomite, calcite, silicified carbonates) composed of carbonate C, Mg, Ca, and Si (± Mn); tentatively organic matter-hosted elements (and/or sulfide-sulfate phases) composed of Cu (± organic C, Zn, Mn Si, Ni, Hg, and Li). Selenium shows a dominant association with the shale component, but correlations and Q-mode factors also indicate that organic matter (within the shale component) and carbonate fluorapatite may host a portion of the Se. Consideration of larger numbers of factors in Q-mode analysis indicates that native Se (a factor containing Se (± Ba)) may also comprise a minor component of the Se compliment.

INTRODUCTION

We have initiated a study of the Rex Chert, which conformably overlies the Meade Peak Phosphatic Shale Member of the Permian Phosphoria Formation. It comprises part of the overburden that is removed to reach the phosphate ore at mines in SE Idaho and therefore comprises a part of the waste dumps. In addition, the Rex Chert is used to surface roads in the mining district. It has been proposed that the chert be used to cap and isolate waste dumps to prevent the release of selenium (Se) and other potentially toxic elements to the environment. Previous spot analyses indicated that Se might occur in high concentrations in some chert beds, so we sampled several outcrop sections to determine the composition of the Rex Chert. A parallel report has been produced by Herring et al. (2002) on channel samples through the Rex Chert from the active Rasmussen Ridge and Enoch Valley phosphate mines. Those channel samples comprise a continuous composite record of Rex Chert composition through the entire section. In contrast, our outcrop samples provide the compositions of a series of individual beds through each outcrop section, with intervening beds being unsampled. One outcrop section sampled also includes the overlying, informally named, cherty shale member of the Phosphoria Formation and another section includes the upper part of the Meade Peak Phosphatic Shale Member and the transition zone between the Meade Peak and Rex Chert.

Background

U.S. Geological Survey (USGS) geologists have studied the Phosphoria Formation in SE Idaho and the Western U.S. Phosphate Field throughout much of the twentieth century. In response to a request by the U.S. Bureau of Land Management (BLM), a new series of resource and geoenvironmental studies was initiated by the USGS in 1998. Present studies involve many scientific disciplines within the USGS and consist of: (1) integrated, multidisciplinary research directed toward resource and reserve estimations of phosphate in selected 7.5-minute quadrangles; (2) element residences, mineralogical and petrochemical characteristics; (3) mobilization and reaction pathways, transport, and disposition of potentially toxic trace elements associated with the occurrence, development, and use of phosphate rock; (4) geophysical signatures; and (5) improving our understanding of the depositional origin and evolution of the deposit.

To carry out these studies, the USGS formed cooperative research relationships with the BLM and the U.S. Forest Service (USFS), which are responsible for land management and resource conservation on public lands, and with five private companies currently leasing or developing phosphate resources in southeastern Idaho. These companies include Nu-West (Agrium U.S. Inc.) (Rasmussen Ridge mine), Astaris Production LLC (Dry Valley mine), Rhodia Inc. (Wooley Valley mine-inactive), J.R. Simplot Co. (Smoky Canyon mine), and P4 Production LLC (Monsanto and Solutia) (Enoch Valley mine). Because raw data acquired during the project will require time to interpret, data are released in open-file reports for prompt availability to other workers. The open-file reports associated with this series of resource and geoenvironmental studies are submitted to each of the Federal and industry collaborators for technical comment; however, the USGS is solely responsible for the data contained in the reports.

Location and General Geology

Ten sections of Rex Chert located in the vicinity of Dry Valley, northeast of Soda Springs in SE Idaho (Fig. 1; Table 1), were described in the field. Three of those sections (1, 5, 7) were measured (Figs. 2-4) and sampled in detail for chemical, mineralogical, and petrographic analyses. This region of SE Idaho has supported extensive phosphate mining over the past several decades and currently has four active mines. Service (1966) evaluated

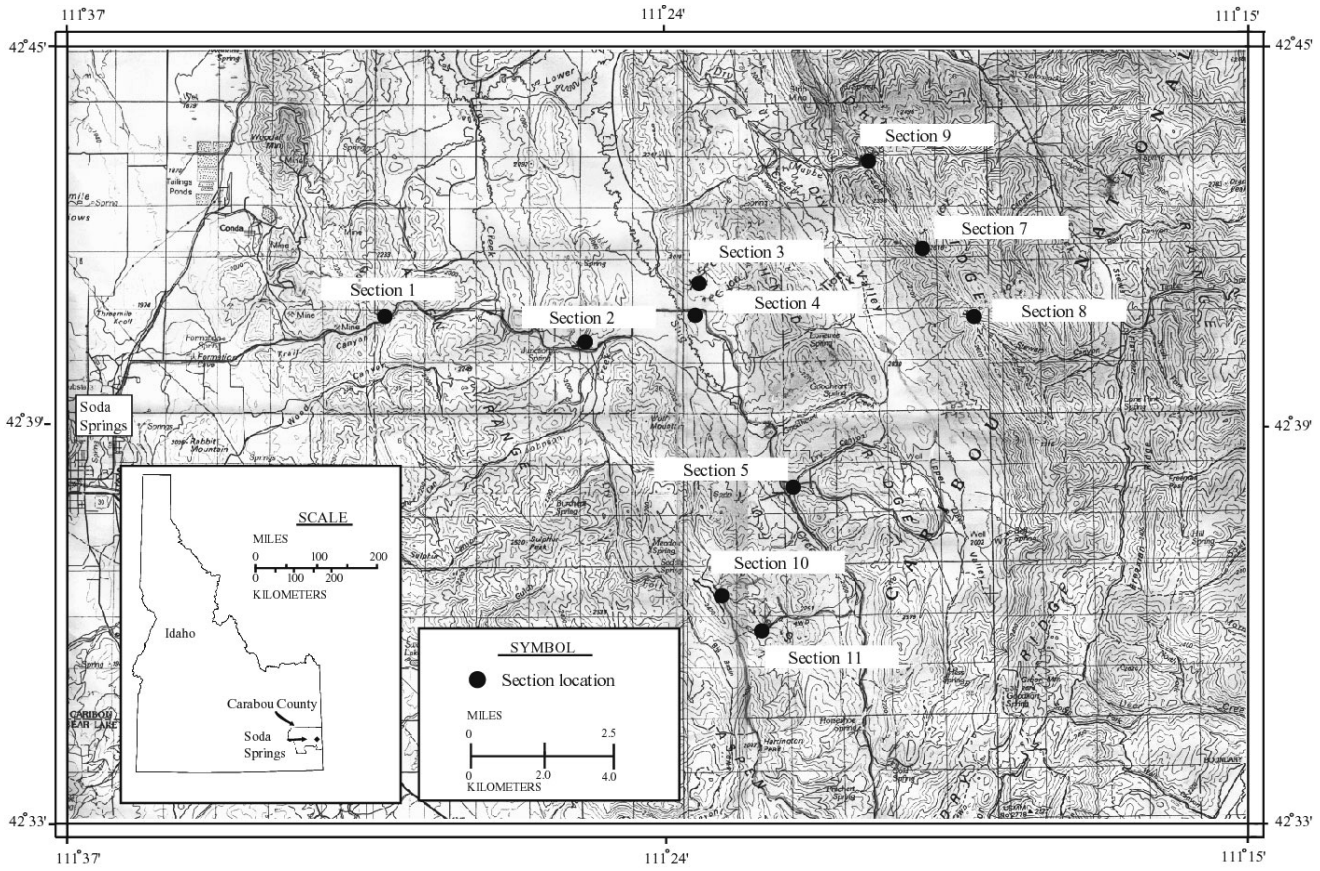

Figure 1. Index map of S. E. Idaho and location of sections of Rex Chert (1-5, 7-11); section 1, 5, and 7 were measured and sampled

Table 1. GPS coordinates and elevations; both accurate within <15 meters (49 ft)

Section Number	Latitude (N)	Longitude (W)	Elevation (m)
Section 1	42° 42.16'	111° 29.07'	2122
Section 2	42° 41.78'	111° 24.61'	1967
Section 3	42° 42.82'	111° 21.93'	1974
Section 4	42° 42.17'	111° 22.04'	1961
Section 5 [1]	42° 39.38'	111° 19.76'	2042
Section 5 [2]	42° 39.39'	111° 19.42'	2042
Section 7	42° 43.91'	111° 17.37'	2248
Section 8	42° 42.15'[3]	111° 17.07'[3]	2560[3]
Section 9	42° 44.85'	111° 17.79'	2100
Section 10	42° 37.55'	111° 21.13'	2314
Section 11	42° 36.89'	111° 20.25'	2134

[1] SW end, [2] NW end, [3] taken from topographic map

the western phosphate industry in Idaho and provided a brief description of the mining history, ore occurrence, and geology, which has recently been updated by Lee (2001). McKelvey and others (1959) discussed in detail the Phosphoria Formation in the Western Phosphate Field. Cressman and Swanson (1964) provided detailed stratigraphy and petrology of these same rock units located in nearby SW Montana. Gulbrandsen and Krier (1980) discussed general aspects of the large and rich phosphate resources of the Phosphoria Formation in the vicinity of Soda Springs. Gulbrandsen (1966, 1975, 1979) summarized bulk chemical compositions for various rock types of the phosphatic intervals of the Phosphoria Formation.

Lithostratigraphy

Three stratigraphic sections of the Rex Chert Member were measured and those three sections along with seven others were described in the field in SE Idaho (Fig. 1). Samples were collected from the three measured sections and their stratigraphic positions are indicated in Fig. 2.

The Phosphoria Formation in the Soda Springs area of SE Idaho consists of three members, which in ascending order are the Meade Peak Phosphatic Shale Member, the Rex Chert, and the informally named cherty shale (McKelvey and others, 1959; Montgomery and Cheney, 1967; Brittenham, 1976; Oberlindacher, 1990). The measured sections of this report focus on the Rex Chert in addition to the cherty shale member in one measured section. The Meade Peak unconformably overlies the Grandeur Tongue of the Permian Park City Formation, and the cherty shale member of the Phosphoria is overlain by the Triassic Dinwoody Formation.

The contacts between the Meade Peak and the Rex Chert and between the Rex Chert and the cherty shale member are gradational. The transitional rocks generally contain carbonates or carbonate-rich beds.

Section 1 was measured through a road cut that exposed the transition zone between the upper part of the Meade Peak and the Rex Chert and an adjacent quarry wall that exposed the cherty shale member. Section 5 was measured in a small quarry where the Rex Chert was being mined for surfacing roads. The underlying Meade Peak was not exposed and the overlying cherty shale was not present. Section 7 was measured along the exposed face of the now-abandoned South Maybe Canyon Mine and includes the upper Meade Peak rocks and transition rocks to the Rex Chert. Measurements record true thickness of strata.

In section 1, the Meade Peak Member is covered and the lowermost beds exposed include limestone alternating with black chert (Fig. 2, unit A). Most of the lower part of the Rex Chert is thin-bedded black and gray chert, which gives way up section to thick-bedded massive gray chert (units B-F). Load casts are seen at the base of the thick chert. The uppermost massive chert beds are composed of composite beds displaying pinch-and-swell structures (unit F). Above the uppermost massive thick chert bed are several thin, iron-rich, weathered chert beds (unit G). Sponge spicules are clearly seen in some of the chert beds, but thin sections reveal that most of the Rex Chert in this section is spicularite. The transition to the overlying cherty shale member is covered in the measured section, but in the outcrop on the opposite (south) side of the road, that position may be occupied by a chert-pebble conglomerate that is not seen on the north side of the road. The lower third of the cherty shale member consists of thin-bedded (up to 6 cm) siliceous shale, with some beds displaying load casts (unit H1). Beds generally thicken up section. The middle third of the section consists of thin-bedded (6-15 cm) argillaceous chert with thinner (<1-3 mm) interbedded siliceous shale (unit H2). The upper third of the section is variable and consists of moderately thick-bedded (10-30 cm) argillaceous chert with sheared siliceous shale partings (unit H3). Near the top of the section occurs a body of pale-brown siliceous dolostone that appears to be the hinge of a fold and the remainder of the bed(?) is not exposed laterally from that body. This was probably originally a dolostone bed or laterally

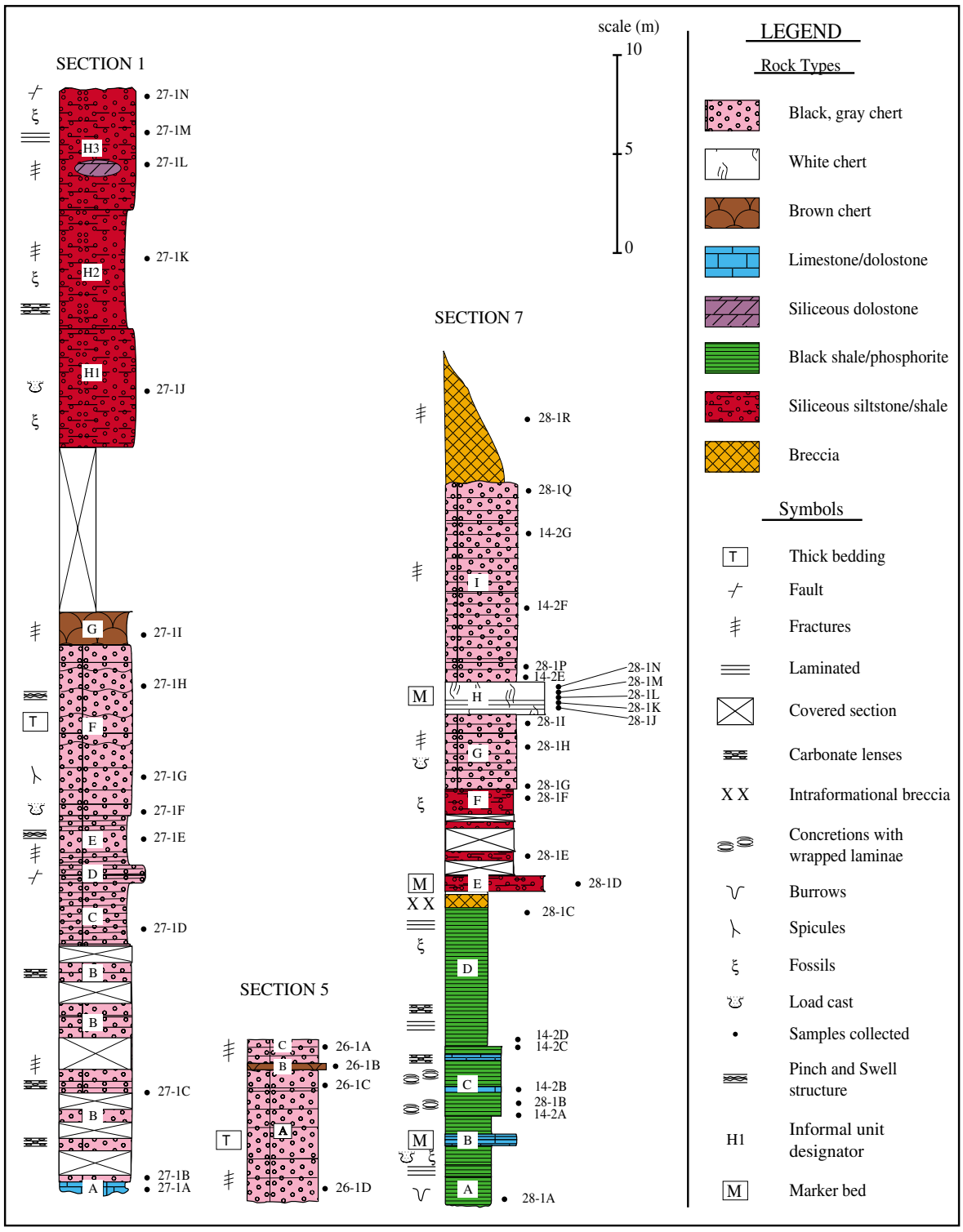

Figure 2. Measured and sampled sections of Rex Chert; units H1-H3 in section 1 is cherty shale member, units A-D in section 7 is Meade Peak Member

extensive lens. A bed (40 cm thick) of laminated and sheared black siliceous shale occurs near the top of the section, which is capped by a nodular siliceous shale bed. The upper part of the section is highly sheared and is likely bounded by a fault. It is likely that the thickness of the Rex Chert and cherty shale members have been altered by folding and faulting. Bedding (S_0) in much of the Rex Chert has been obscured by development of generally low-relief stylolites (S_1) oriented subparallel to bedding. Locally, bedding has been transposed (S_2) so that it parallels axial planes of isoclinal folds that may have formed during compaction, or possibly during emplacement of the Paris thrust plate. S_2 remained an active structural element as shown by quartz veins that formed perpendicular to S_2 and are offset along S_2.

Section 5 was measured at its NW end in a quarry where the thickness of the Rex Chert is a minimum because the lower part of the section is covered and the upper part has been removed by quarrying. The Rex Chert consists of dark-gray, medium- to thick-bedded chert that is divided into two sections by an intervening friable brown layer of ferruginous chert (unit B) that has an earthy texture. This 30-40 cm-thick brown zone may be alteration along a fault or leaching of a chert bed. The cherts in this section are spicularites, as determined from thin sections. The chert shows bedding-parallel pressure-solution cleavage as indicated by truncated microfossils and accumulations of relatively insoluble components such as sericite and hematite.

In section 7, the upper part of the Meade Peak Member (units A-D) and the transition to the Rex Chert (units E-F) are well exposed. Alternating beds of black shale, phosphorite, and carbonate characterize the Meade Peak exposure. Carbonates (calcite and dolomite) occur as beds, horizons of disconnected concretions, and as isolated concretions in some shale beds. Generally the carbonates thicken up section from nodules to thin beds to thicker beds, except near the base of the exposed section where a 0.6 m thick carbonate "marker bed" occurs. These marker beds (see below also) crop out over a distance of about 3 miles (4.8 km) in the North, Middle, and South Maybe Canyon mines in the Dry Ridge Mountains. Shale and phosphorite laminae wrap around the carbonate concretions indicating an early diagenetic origin (pre-compaction). The Meade Peak is overlain by a 0.8 m thick marker bed of siliceous siltstone (Fig. 2, unit E). That bed is overlain by a section that is partly covered, but consists predominantly of thin-bedded siliceous siltstone (unit F). That transition zone of siliceous siltstones is overlain by thin- to medium-bedded (5-30 cm) black chert with brown upper and lower margins on each bed (unit G). Load casts are seen at the base of some beds. A few thin siliceous siltstone beds also occur in unit G. Those cherts are overlain by 1 m of thin-bedded white chert that is overlain by a 1 m thick white chert marker bed (unit H). The white cherts are overlain by 10 m of thin- to medium-bedded (to 30 cm) black and gray chert (unit I) that is very similar to cherts in unit G. The section is capped by a 8 m thick, discontinuous chert megabreccia with a calcite-bearing quartz cement. This breccia body may be a slump deposit or fault-zone deposit.

METHODS

Field Sampling

The samples within the measured sections obtained for analyses were collected as individual beds, where possible. In several places, where beds were too thick to collect in their entirety, portions of beds were collected. This approach provides an opportunity to determine the changes in composition of like samples through the history of deposition of stratigraphic sections. The choice of beds sampled is intended to provide uniform representation of each section. In addition, unusual rock types were sampled, for example

a large dolomitic body in the cherty shale member. About 0.1-1 kg of rock was collected for each bed.

Rock Sample Preparation

A representative slab was cut through the entire thickness of each chert bed sample and was crushed in a mechanical jaw crusher, and then powdered in a roller mill. An aliquot of the powdered material was analyzed by X-ray diffraction for mineral content and a second aliquot was sent to a contract laboratory for chemical analyses. All splits were obtained with a riffle splitter to ensure similarity with the whole sample. Splits of about 15-50 g were sent to the contract laboratory and the remaining powders for all samples are archived at the USGS. A second slab of each chert bed sample was cut into one or more thin sections for petrographic analysis.

Analyses

Samples were analyzed for 40 major, minor, and trace elements using acid digestion in conjunction with inductively coupled plasma-atomic emission spectrometry (ICP-AES). For the 40-element analysis (referred to as ICP-40), a split was dissolved using a low-temperature (<150° C) digestion with concentrated hydrochloric, hydrofluoric, nitric, and perchloric acids (Jackson and others, 1987). The analytical contractor modified this procedure to shorten the digestion time (P. Lamothe, USGS, oral communication). The acidic sample solutions were taken to dryness and the residue was dissolved with 1 ml of aqua regia and then diluted to 10.0 g with 1% (volume/volume) nitric acid. Strontium and Ba concentrations were determined by both ICP-40 and ICP-16 (see below) techniques and the two data sets are comparable (R^2 = 0.999 for Sr and 0.997 for Ba) and are reported in Table 3. Manganese concentrations were also provided by both ICP techniques and they have comparable accuracy and precision, however, the ICP-40 data set is the only one reported because it has a much lower detection limit, 4 parts per million (ppm) compared to 100 ppm for ICP-16. The ICP-40 technique measures the following elements above the indicated ppm limits: Au 8 ppm, Bi 50 ppm, Sn 50 ppm, Ta 40 ppm, and U 100 ppm; however, no samples had concentrations above those quantification limits and those elements are not included in Table 3.

Another split of the each sample was fused with lithium metaborate then analyzed by ICP-AES after acid dissolution of the fusion mixture. This technique, referred to as ICP-16, provides analysis of all major elements, including Si, and a few minor and trace elements. Cherts are very high silica rocks yet the accuracy of Si determinations is quite good, probably about 2-4% based on the total-oxide sums. Si measurement is not possible using the 4-acid digestion ICP-40 technique because it is lost as a volatile fluoride compound during digestion. Analysis of major elements using the fusion technique also provides a compositional check on the concentrations of these same elements as measured by acid digestion. Titanium and Cr were analyzed using both ICP techniques, but only data from the ICP 16 technique are given in Table 3 because the fusion technique more completely digests resistant minerals that might contain those elements.

Selenium concentrations were determined using hydride generation followed by atomic absorption (AA) spectrometry. Selenium is not reported using either of the ICP techniques, as it is generally volatilized during sample preparation. The hydride generation combined with AA technique was also used to determine concentrations of As, Sb, and Tl. The hydride analytical technique is considered to be more sensitive than the acid digestion ICP-AES analytical technique for As and are the data reported here. Mercury was determined by cold vapor atomic absorption spectrometry.

Total S and total C were measured using combustion in oxygen followed by infrared measurement of the evolved gas. For the other forms of carbon, carbonate carbon was

Table 3. Chemical composition of rocks from three sections (1, 5, 7; Figs. 1, 2) of Rex Chert and adjacent rocks; samples are listed in stratigraphic order; major oxides, C, and S in wt.%, others in ppm

Lab No.	Sample No.	Sample Description	Lithology	SiO2 ICP-16	Al2O3 ICP-16	Fe2O3 ICP-16	TiO2 ICP-16	CaO ICP-16	K2O ICP-16	MgO ICP-16	Na2O ICP-16	P2O5 ICP-16
SECTION 1: REX CHERT 1A-1I; CHERTY SHALE MEMBER 1J-1N												
C-197024	601-27-1N	Brown, calcareous	Cherty-calcareous shale bed	87.5	3.27	0.77	0.22	2.28	0.61	1.09	0.63	0.48
C-197023	601-27-1M	Black	Laminated siliceous shale	78.7	8.41	2.66	0.55	1	1.95	0.8	0.59	0.7
C-197022	601-27-1L2	Pale brown to gray=fresh	Siliceous dolostone	48.8	1.1	0.7	0.07	16.2	0.16	9.91	0.22	0.16
C-197021	601-27-1L1	Brown, earthy, porous	Argillaceous chert bed	92.6	2.74	1.92	0.17	0.43	0.3	0.18	0.61	0.32
C-197020	601-27-1K2	Brown, calcareous	Argillaceous chert bed	92	2.4	0.64	0.17	1.41	0.43	0.73	0.31	0.2
C-197019	601-27-1K	Brown	Shaly interbed	90.9	3.48	0.96	0.23	0.8	0.64	0.32	0.42	0.44
C-197018	601-27-1J	Brown, calcareous	Cherty shale bed	86.2	3.82	1.16	0.23	2.01	0.78	0.95	0.49	0.44
C-197017	601-27-1I	Brown, Fe stained	Phosphatic-ferruginous chert bed	83.2	2.55	4.68	0.12	3.69	0.64	0.45	0.08	3.05
C-197016	601-27-1H	Gray	Chert bed	98.2	0.79	0.76	0.02	0.5	0.13	0.07	0.04	0.37
C-197015	601-27-1G	Gray, spicular	Base of massive thick chert bed	95.6	1.19	1.4	0.03	0.97	0.22	0.12	0.03	0.85
C-197014	601-27-1F	Gray	Chert bed	99.9	0.26	0.23	<0.02	0.39	0.02	<0.02	0.01	0.28
C-197013	601-27-1E	Gray	Chert bed	96	0.62	0.44	<0.02	1.27	0.08	0.05	0.03	0.96
C-197012	601-27-1D	Black	Chert bed	98.2	0.6	0.33	0.02	0.21	0.1	0.05	0.04	0.09
C-197011	601-27-1C	Black, calcareous	Chert bed	97.5	0.43	0.19	0.02	1.1	0.06	0.18	0.04	0.16
C-197010	601-27-1B	Black, calcareous	Chert bed	93.5	0.59	0.17	0.03	2.31	0.07	0.93	0.05	0.28
C-197009	601-27-1A	Gray	Siliceous limestone bed	44.3	0.2	0.06	<0.02	30.9	0.04	0.48	0.04	0.05
SECTION 5												
C-197005	601-26-1A	Dark gray, fractured	Chert bed	98.6	0.55	0.31	0.02	0.22	0.07	0.05	0.04	0.14
C-197006	601-26-1B	Earthy, brown	Leached zone in chert	93.9	1.49	2.65	0.08	0.43	0.17	0.12	0.04	0.3
C-197007	601-26-1C	Dark gray, fractured	Chert bed	97.5	1.04	0.47	0.03	0.29	0.16	0.1	0.05	0.18
C-197008	601-26-1D	Dark gray, fractured	Chert bed	97.5	1.1	0.49	0.05	0.25	0.18	0.08	0.07	0.14
SECTION 7: MEADE PEAK 601-28-1A-1C: REX CHERT 601-28-1D THROUGH 601-28-1R1												
C-197045	601-28-1R1	Pale brown-gray chert clast	Breccia	99.5	0.4	0.07	<0.02	1.05	0.05	0.55	0.05	0.14
C-197044	601-28-1Q	Dark gray, fractured	Chert bed	101	0.4	0.06	<0.02	0.46	0.04	0.02	0.05	0.28
C-205123	502-14-2G	Gray	Chert bed	95.1	0.55	0.11	0.03	0.41	0.05	0.02	0.08	0.25
C-205122	502-14-2F	Black, fractured	Chert bed	95.81	0.6	0.11	0.03	0.43	0.06	0.03	0.08	0.25
C-205121	502-14-2E	Brown	Chert bed	94.29	0.72	0.21	0.03	0.49	0.08	0.03	0.07	0.3
C-197043	601-28-1P	Gray, mottled	Chert bed	96.7	0.25	0.04	<0.02	2.92	0.01	0.7	0.04	0.09
C-197042	601-28-1N	White, upper 15 cm margin	1N-1K=parts of a 80 cm thick	102	0.28	0.17	<0.02	0.3	0.04	0.02	0.04	0.18
C-197041	601-28-1M	White, middle 7 cm	white chert bed	101	0.32	0.04	<0.02	0.18	0.01	0.02	0.03	0.09
C-197040	601-28-1L	White, 7-15 cm above base	chert	101	0.23	0.13	<0.02	0.27	<0.01	0.02	0.03	0.16
C-197039	601-28-1K	White, lower margin (8 cm)	chert	101	0.36	0.1	<0.02	0.35	0.02	0.02	0.03	0.2
C-197036	601-28-1J1	Pale brown, upper bed margin	Chert	100	0.28	0.1	<0.02	0.3	0.02	0.02	0.04	0.18
C-197037	601-28-1J2	White-gray, main bed, dense	Chert	101	0.32	0.04	<0.02	0.2	0.02	<0.02	0.03	0.11
C-197038	601-28-1J3	White-gray, lower bed margin	Chert	101	0.42	0.09	<0.02	0.34	0.02	0.02	0.03	0.21
C-197035	601-28-1I	Black-brown	Chert bed	96.7	0.77	0.21	0.03	0.5	0.1	0.03	0.08	0.32
C-197034	601-28-1H	Pale brown, silty	Chert bed	99.5	0.43	0.17	0.02	0.34	0.05	0.03	0.07	0.2
C-197031	601-28-1G1	Pale brown, upper bed margin	Chert	96	1.38	0.37	0.05	1.01	0.22	0.08	0.12	0.7
C-197032	601-28-1G2	Brown, main bed	Chert	90.7	0.93	0.26	0.05	0.67	0.14	0.05	0.11	0.39
C-197033	601-28-1G3	Pale brown, lower bed margin	Chert	95.4	1.64	0.6	0.08	1.48	0.27	0.12	0.12	1.01

Table 3 continued

Lab No.	Sample No.	Sample Description	Lithology	SiO2 ICP-16	Al2O3 ICP-16	Fe2O3 ICP-16	TiO2 ICP-16	CaO ICP-16	K2O ICP-16	MgO ICP-16	Na2O ICP-16	P2O5 ICP-16
C-197030	601-28-1F	Gray-brown, fossiliferous	Phosphatic cherty shale bed	89	3.48	1.24	0.18	2.46	0.69	0.3	0.15	1.72
C-197029	601-28-1E	Black, thin-bedded	Siliceous siltstone	75	10.7	2.09	0.78	0.17	2.58	0.65	1.2	0.09
C-197028	601-28-1D	Gray-brown, mid. Thick bed	Siliceous siltstone, marker bed	78.5	11.1	0.96	0.82	0.34	2.57	0.61	1.32	0.05
C-197027	601-28-1C	Black	Phosphatic-calcareous shale	48.3	8.35	2.75	0.48	17.1	1.88	0.7	0.66	5.5
C-205120	502-14-2D	Black, carbonaceous	Phosphorite	3.96	0.59	0.13	0.03	46.8	0.12	0.07	0.16	33.1
C-205119	502-14-2C	Black nodule	Carbonate nodule in black shale	3.53	0.47	0.16	0.03	47.8	0.08	2.74	0.22	2.82
C-205118	502-14-2B	Black, carbonaceous	Phosphatic shale	16.1	2.48	0.81	0.13	35.1	0.65	0.91	0.63	15.4
C-197026	601-28-1B	Black nodule	Carbonate nodule in black shale	1.1	0.15	0.06	<0.020	48.7	0.01	3.3	0.11	2.8
C-205117	502-14-2A	Black, carbonaceous	Phosphatic shale	23.8	3.87	1.3	0.23	31.5	0.96	1.09	0.74	9.56
C-197025	601-28-1A	Black, carbonaceous	Phosphatic shale	46	7.29	2.37	0.48	11.1	1.94	1.44	1.2	4.42

Sample No. Section 1	∑CO2 Acid.	Total --	CT Comb.	C C Acid.	Corg. Difference	ST Comb.	Ag ICP-40	As Hydride	Ba ICP-40	Ba ICP-16	Be ICP-40	Cd ICP-40	Ce ICP-40	Co ICP-40
601-27-1N	1.69	98.6	1.32	0.46	0.86	0.2	<2	3.1	593	611	<1	<2	19	<2
601-27-1M	0.03	95.4	1.81	0.01	1.8	0.05	<2	12.6	243	243	2	<2	36	3
601-27-1L2	23.4	101	6.36	6.39	-0.03	<0.05	<2	1.1	28	27	<1	<2	6	<2
601-27-1L1	0.02	99.3	0.11	0.01	0.1	<0.05	<2	3.8	57	60	<1	<2	12	<2
601-27-1K2	1.15	99.5	0.77	0.31	0.46	0.12	<2	2.5	480	439	<1	<2	13	<2
601-27-1K	0.23	98.5	0.76	0.06	0.7	<0.05	<2	3.8	138	125	<1	<2	19	2
601-27-1J	1.58	97.7	1.57	0.43	1.14	0.07	<2	3.1	123	124	<1	<2	20	3
601-27-1I	0.08	98.5	0.31	0.02	0.29	<0.05	<2	13.2	78	81	2	<2	87	<2
601-27-1H	0.02	100	0.13	0.01	0.12	<0.05	<2	6.1	86	80	<1	<2	9	<2
601-27-1G	0.02	100	0.13	0.01	0.12	<0.05	<2	5.1	39	48	<1	<2	10	<2
601-27-1F	0.01	101	0.01	<0.003	0.007	<0.05	<2	0.9	18	16	<1	<2	<5	<2
601-27-1E	0.02	99.7	0.27	0.01	0.26	<0.05	<2	2.5	30	30	<1	<2	<5	<2
601-27-1D	0.03	99.7	0.39	0.01	0.38	<0.05	<2	1.3	50	49	<1	<2	<5	<2
601-27-1C	0.79	100	0.38	0.22	0.16	<0.05	<2	0.7	26	27	<1	<2	<5	<2
601-27-1B	2.2	100	0.91	0.59	0.32	<0.05	<2	1	25	24	<1	<2	<5	<2
601-27-1A	25.1	101	7.06	6.85	0.21	<0.05	<2	<0.6	8	<10	<1	<2	<5	<2
Section 5														
601-26-1A	0.02	100	0.09	0.01	0.08	<0.05	<2	1.6	273	261	<1	<2	<5	<2
601-26-1B	0.01	99.2	0.11	<0.003	0.107	<0.05	<2	14.5	85	84	<1	<2	8	<2
601-26-1C	0.03	99.9	0.13	0.01	0.12	<0.05	<2	2.7	127	115	<1	<2	5	<2
601-26-1D	0.01	99.9	0.19	<0.003	0.187	0.05	<2	2.4	423	415	<1	<2	6	<2
Section 7														
601-28-1R1	1.1	102	0.38	0.3	0.08	<0.05	<2	4.3	27	32	<1	<2	<5	<2
601-28-1Q	0.02	102	0.11	0.01	0.1	<0.05	<2	5.4	25	26	<1	<2	<5	<2
502-14-2G	0.03	96.6	0.09	0.01	0.08	<0.05	<2	3.7	31	35	<1	<2	<5	<2
502-14-2F	0.02	97.4	0.17	0.01	0.16	<0.05	<2	1.1	39	37	<1	<2	<5	<2
502-14-2E	0.02	96.3	0.05	0.01	0.04	<0.05	<2	2.2	63	64	<1	<2	<5	<2
601-28-1P	2.78	103	0.81	0.76	0.05	<0.05	<2	<0.6	17	23	<1	<2	<5	<2
601-28-1N	0.01	103	0.02	<0.003	0.017	<0.05	<2	0.9	21	28	<1	<2	<5	<2
601-28-1M	0.01	102	0.01	<0.003	0.007	<0.05	<2	<0.6	24	26	<1	<2	<5	<2

Table 3 continued

Sample No. Section 7	∑CO2 Acid.	Total --	CT Comb.	CC Acid.	Corg. Difference	ST Comb.	Ag ICP-40	As Hydride	Ba ICP-40	Ba ICP-16	Be ICP-40	Cd ICP-40	Ce ICP-40	Co ICP-40
601-28-1L	0.01	102	0.03	<0.003	0.027	<0.05	<2	2.8	21	22	<1	<2	<5	<2
601-28-1K	0.02	102	0.02	0.01	0.01	<0.05	<2	0.9	25	33	<1	2	<5	<2
601-28-1J1	<0.01	101	0.03	<0.003	0.027	<0.05	<2	2.3	35	37	<1	2	<5	<2
601-28-1J2	<0.01	102	0.02	<0.003	0.017	<0.05	<2	0.8	39	44	<1	<2	<5	<2
601-28-1J3	0.01	102	0.03	<0.003	0.027	<0.05	7	1.2	37	40	<1	<2	<5	<2
601-28-1I	0.02	98.8	0.15	0.01	0.14	<0.05	<2	2.1	43	43	<1	<2	<5	<2
601-28-1H	0.02	101	0.12	0.01	0.11	<0.05	<2	0.6	29	33	<1	<2	8	<2
601-28-1G1	0.05	100	0.18	0.01	0.17	<0.05	3	6.6	51	50	<1	4	7	<2
601-28-1G2	0.02	93.3	0.35	0.01	0.34	0.05	<2	4.1	62	56	<1	4	5	<2
601-28-1G3	0.07	101	0.21	0.02	0.19	<0.05	3	11	62	59	<1	11	10	<2
601-28-1F	0.11	99.3	0.18	0.03	0.15	<0.05	3	16.8	108	108	1	22	19	<2
601-28-1E	<0.01	93.1	3.35	<0.003	3.347	0.42	<2	14.2	342	336	1	<2	47	<2
601-28-1D	<0.01	96.3	0.76	<0.003	0.757	0.18	6	1.9	365	351	1	7	46	<2
601-28-1C	8.18	93.9	4.62	2.23	2.39	0.29	<2	23.2	367	346	1	5	62	8
502-14-2D	1.45	86.4	8.84	0.4	8.44	1.08	<2	3.8	56	49	1	79	21	<2
502-14-2C1	38.7	96.6	12.1	10.6	1.54	0.28	<2	2.5	22	17	<1	22	6	<2
502-14-2B	12.3	84.5	13.8	3.36	10.4	1.86	8	26.7	88	91	1	35	29	3
601-28-1B	39.3	95.4	13.8	10.7	3.07	0.27	<2	3.3	14	11	<1	15	<5	<2
502-14-2A	12.8	85.8	15.7	3.49	12.2	2.52	14	42.5	108	106	2	194	27	2
601-28-1A	5.49	81.7	13.3	1.5	11.8	2.97	15	32.2	223	212	2	37	52	4

Sample No. Section 1	Cr ICP-16	Cu ICP-40	Eu ICP-40	Ga ICP-40	Hg CVAA	Ho ICP-40	La ICP-40	Li ICP-40	Mn ICP-40	Mo ICP-40	Nb ICP-40	Nd ICP-40	Ni ICP-40	Pb ICP-40	Sb Hydride
601-27-1N	172	32	<2	<4	0.05	<4	20	14	81	<2	<4	25	37	9	0.7
601-27-1M	759	56	<2	14	0.15	<4	31	27	76	<2	<4	37	97	7	0.6
601-27-1L2	95	29	<2	<4	0.02	<4	8	16	298	<2	6	10	14	4	<0.6
601-27-1L1	137	20	<2	<4	0.04	<4	10	29	333	<2	<4	13	45	<4	<0.6
601-27-1K2	139	23	<2	<4	0.04	<4	10	17	68	3	<4	14	29	5	<0.6
601-27-1K	224	49	<2	4	0.03	<4	16	13	60	<2	<4	22	40	7	0.6
601-27-1J	300	31	<2	5	0.03	<4	17	12	91	<2	<4	22	44	6	0.9
601-27-1I	1100	36	8	8	0.14	7	176	43	31	<2	4	197	21	13	2.2
601-27-1H	106	13	<2	<4	0.02	<4	18	8	13	<2	<4	21	10	<4	<0.6
601-27-1G	170	23	<2	<4	0.04	<4	14	8	16	<2	<4	30	13	<4	<0.6
601-27-1F	23	11	<2	<4	<0.02	<4	12	5	16	<2	<4	12	4	<4	<0.6
601-27-1E	67	27	<2	<4	0.05	<4	19	6	38	<2	<4	23	21	<4	<0.6
601-27-1D	86	152	<2	<4	0.04	<4	3	9	42	2	<4	<9	20	9	0.6
601-27-1C	19	33	<2	<4	<0.02	<4	3	4	37	<2	<4	<9	8	<4	<0.6
601-27-1B	39	30	<2	<4	<0.02	<4	7	4	50	<2	<4	<9	11	<4	<0.6
601-27-1A	12	24	<2	<4	<0.02	<4	3	4	148	<2	<4	<9	4	4	<0.6
Section 5															
601-26-1A	51	24	<2	<4	0.02	<4	5	6	29	<2	<4	<9	8	<4	0.9
601-26-1B	72	60	<2	<4	0.1	<4	10	10	1710	<2	<4	15	98	5	1
601-26-1C	81	32	<2	<4	0.03	<4	4	13	36	<2	<4	11	11	<4	0.7

Table 3 continued

Sample No.	Cr	Cu	Eu	Ga	Hg	Ho	La	Li	Mn	Mo	Nb	Nd	Ni	Pb	Sb
Section 5	ICP-16	ICP-40	ICP-40	ICP-40	CVAA	ICP-40	ICP-40	ICP-40	ICP-40	ICP-40	ICP-40	ICP-40	ICP-40	ICP-40	Hydride
601-26-1D	74	13	<2	<4	0.03	<4	6	10	22	<2	<4	9	13	<4	0.7
Section 7															
601-28-1R1	15	9	<2	<4	<0.02	<4	3	5	106	<2	<4	<9	6	<4	0.8
601-28-1Q	12	6	<2	<4	<0.02	<4	3	4	21	<2	<4	<9	5	<4	<0.6
502-14-2G	16	5	<2	<4	<0.02	<4	7	4	48	<2	<4	<9	6	<4	<0.6
502-14-2F	36	8	<2	<4	0.03	<4	9	4	23	<2	<4	<9	7	<4	<0.6
502-14-2E	50	5	<2	<4	0.02	<4	9	6	143	<2	<4	<9	16	<4	<0.6
601-28-1P	<10	10	<2	<4	<0.02	<4	3	4	160	<2	<4	<9	23	<4	<0.6
601-28-1N	20	148	<2	<4	<0.02	<4	5	5	92	<2	<4	<9	8	<4	<0.6
601-28-1M	<10	8	<2	<4	<0.02	<4	3	<2	57	<2	<4	<9	4	<4	<0.6
601-28-1L	10	93	<2	<4	<0.02	<4	4	3	191	<2	<4	<9	10	<4	<0.6
601-28-1K	15	40	<2	<4	<0.02	<4	6	13	221	<2	<4	<9	11	<4	<0.6
601-28-1J1	12	122	<2	<4	<0.02	<4	4	4	299	<2	<4	<9	20	<4	1
601-28-1J2	11	7	<2	<4	<0.02	<4	3	4	250	<2	<4	<9	15	<4	<0.6
601-28-1J3	13	12	<2	<4	<0.02	<4	6	7	227	<2	<4	<9	21	<4	<0.6
601-28-1I	48	10	<2	<4	0.03	<4	9	6	48	<2	<4	<9	13	<4	0.7
601-28-1H	13	33	<2	<4	0.03	<4	6	6	107	<2	<4	<9	13	58	11.4
601-28-1G1	148	154	<2	<4	0.04	<4	18	12	55	<2	<4	13	31	6	1
601-28-1G2	102	34	<2	<4	0.06	<4	12	8	51	2	<4	<9	29	<4	<0.6
601-28-1G3	234	296	<2	<4	0.05	<4	29	16	58	<2	<4	21	45	<4	0.8
601-28-1F	601	52	<2	6	0.05	<4	48	18	34	<2	<4	37	86	5	1.5
601-28-1E	452	38	<2	16	0.16	<4	29	21	32	12	<4	18	33	14	1.8
601-28-1D	135	52	<2	13	0.1	<4	26	18	24	<2	5	20	25	13	0.9
601-28-1C	589	67	4	12	0.17	<4	140	21	496	14	5	93	251	13	1.8
502-14-2D	151	36	<2	<4	0.08	<4	92	3	10	6	<4	57	40	13	<0.6
502-14-2C1	73	17	<2	<4	0.03	<4	8	<2	102	7	<4	10	16	6	<0.6
502-14-2B	1180	98	3	<4	0.3	<4	141	7	59	24	4	81	223	12	4.1
601-28-1B	153	41	<2	<4	0.03	<4	11	<2	69	18	4	16	27	6	0.9
502-14-2A	1650	184	<2	8	0.64	<4	86	14	82	117	6	53	387	15	9.2
601-28-1A	1800	183	2	15	0.59	<4	84	31	146	65	11	59	361	14	6.2

Sample No.	Sc	Se	Sr	Sr	Th	Tl	V	Y	Yb	Zn	Zr
Section 1	ICP-40	Hydride	ICP-40	ICP-16	ICP-40	Hydride	ICP-40	ICP-40	ICP-40	ICP-40	ICP-16
601-27-1N	3	2.8	85	92	<6	0.1	32	36	2	110	95
601-27-1M	9	0.9	66	70	7	0.5	86	49	3	154	164
601-27-1L2	<2	0.4	124	126	<6	<0.1	14	13	<1	28	31
601-27-1L1	3	0.9	23	26	<6	0.3	27	20	2	112	70
601-27-1K2	2	1.8	64	65	<6	0.1	20	16	<1	49	72
601-27-1K	4	1.9	52	56	<6	0.1	31	31	2	98	101
601-27-1J	4	2.4	63	65	<6	0.1	37	32	2	99	91
601-27-1I	3	2.2	215	231	<6	0.1	188	321	13	52	42
601-27-1H	<2	0.9	27	30	<6	<0.1	24	30	1	43	<10
601-27-1G	<2	1.2	34	40	<6	0.3	38	54	3	135	18

Table 3 continued

Sample No.	Sc	Se	Sr	Sr	Th	Tl	V	Y	Yb	Zn	Zr
Section 1	ICP-40	Hydride	ICP-40	ICP-16	ICP-40	Hydride	ICP-40	ICP-40	ICP-40	ICP-40	ICP-16
601-27-1F	<2	0.4	16	17	<6	<0.1	4	16	<1	30	<10
601-27-1E	<2	1.9	44	47	<6	<0.1	21	46	2	78	15
601-27-1D	<2	0.8	14	14	<6	<0.1	19	8	<1	133	<10
601-27-1C	<2	<0.2	23	23	<6	<0.1	5	6	<1	57	13
601-27-1B	<2	0.3	34	36	<6	<0.1	14	13	<1	81	16
601-27-1A	<2	<0.2	188	183	<6	<0.1	5	3	<1	32	<10
Section 5											
601-26-1A	<2	0.6	22	23	<6	<0.1	11	10	<1	29	<10
601-26-1B	<2	0.6	24	28	<6	0.3	35	20	1	244	45
601-26-1C	<2	0.5	24	27	<6	<0.1	15	12	<1	45	27
601-26-1D	<2	0.9	51	54	<6	<0.1	18	13	<1	50	23
Section 7											
601-28-1R1	<2	<0.2	19	21	<6	<0.1	5	5	<1	38	12
601-28-1Q	<2	0.2	17	17	<6	<0.1	3	5	<1	24	<10
502-14-2G	<2	0.4	22	22	<6	<0.1	5	10	<1	35	13
502-14-2F	<2	<0.2	21	22	<6	<0.1	9	13	<1	36	22
502-14-2E	<2	0.8	23	24	<6	<0.1	14	13	<1	63	21
601-28-1P	<2	<0.2	15	15	<6	<0.1	<2	4	<1	73	<10
601-28-1N	<2	<0.2	11	15	<6	<0.1	3	7	<1	121	13
601-28-1M	<2	<0.2	8	<10	<6	<0.1	<2	3	<1	28	<10
601-28-1L	<2	<0.2	10	11	<6	<0.1	3	6	<1	109	12
601-28-1K	<2	<0.2	12	13	<6	<0.1	5	8	<1	94	21
601-28-1J1	<2	<0.2	14	15	<6	<0.1	3	6	<1	153	<10
601-28-1J2	<2	<0.2	12	15	<6	<0.1	<2	4	<1	62	<10
601-28-1J3	<2	<0.2	15	17	<6	<0.1	4	8	<1	79	<10
601-28-1I	<2	2.5	29	32	<6	<0.1	13	15	<1	91	14
601-28-1H	<2	0.7	16	17	<6	<0.1	5	9	<1	90	<10
601-28-1G1	<2	1.3	43	46	<6	0.7	47	29	1	253	19
601-28-1G2	<2	2.9	36	35	<6	0.4	27	19	<1	123	13
601-28-1G3	3	1.3	58	60	<6	0.8	63	44	2	437	24
601-28-1F	4	3.8	95	97	<6	0.9	130	76	4	569	52
601-28-1E	8	138	80	83	12	1.3	122	10	2	96	394
601-28-1D	7	101	78	82	9	1	63	9	2	115	397
601-28-1C	9	17.2	275	282	<6	1.1	110	206	10	658	233
502-14-2D	4	114	920	914	<6	2.6	579	191	10	483	62
502-14-2C1	<2	16.8	425	420	<6	0.8	176	13	<1	284	30
502-14-2B	6	57.1	1010	1030	<6	1	486	256	11	1070	114
601-28-1B	<2	6.1	696	699	<6	<0.1	280	21	<1	201	23
502-14-2A	6	83.9	749	788	<6	2.4	586	147	8	3060	134
601-28-1A	9	99.5	437	436	<6	1.1	196	144	8	1460	243

measured as evolved CO_2 after acidification of the sample, and organic carbon was calculated as the difference between total and carbonate carbon. The compilations by Arbogast (1996) and Baedecker (1987) include additional discussions about the various types of analytical methodologies used here.

The concentration of each element is reported in the chemistry table as received from the analysts. However, qualified data (detection limit values) were modified for use in statistical analyses. An element was not used in statistical analyses if more than 30% of the data points for that particular element were qualified. If there were fewer than 30% qualified values for an element, then the qualified values were multiplied by 0.5 and data for that element were used in the statistical analyses.

Mineral compositions were determined by X-ray diffraction using a Philips diffractometer with a graphite monochromator and CuKα radiation. Samples were run from 4-70° 2Θ at 40 kV, 45 mA, and 10 counts per second. Semiquantitative mineral contents were determined and are grouped in Table 2 under the classifications of major (>25%), moderate (5-25%), and minor (<5%).

Statistical analyses were performed on 3 data sets including all data (except data for the Meade Peak in section 7 and the two carbonate beds in section 1); data solely for section 1 and data solely for section 7. The usual Pearson product moment correlation coefficient was used to calculate correlation coefficient matrices. A 99% confidence level was used to calculate the zero-point of correlation. For Q-mode factor analysis, each variable percentage was scaled to the percent of the maximum value before the values were row-normalized and cosine theta coefficients calculated. Factors were derived from orthogonal rotations of principal component eigenvectors using the Varimax method (Klovan and Imbrie, 1971). All communalities are ≥0.90.

RESULTS

Petrography

The dominant characteristic of the chert beds is the presence of sponge spicules, which vary from relatively well preserved to faint ghosts. Most of the chert beds can be classified as spicularites (spongolites). These spicularites are laminated and commonly show a preferred orientation of elongate grains parallel to bedding. One sample (601-28-1H) shows preferred orientation in some laminae but not in others, indicating that the alignment of grains was caused by bottom currents rather than by compaction or tectonics. The sparse to common occurrence of rhombs characterize most spicularite beds. These rhombs are likely quartz-replaced dolomite rhombs. Glauconite, mica, and feldspar are present in some beds. Various combinations of bivalves, fish debris, radiolarians(?), and calcareous algae(?), are seen in some beds. Spicularite beds in section 7 show sedimentary structures that include cross bedding and cut-and-fill scouring.

The upper part of section 7 does not consist of spicularite beds, but rather consist of replaced carbonates. These chert beds are generally white to grayish, centimeters to a meter thick, and in thin section consist of abundant rhombs partly to completely replaced by quartz. Some replaced rhombs show relict carbonate twinning. Laminae are compacted around some large rhombs, which indicates that they formed during early diagenesis prior to compaction. The textures indicate that carbonate and silica fossils were deposited on the seafloor, dolomite rhombs formed in unconsolidated sediment during early diagenesis, compaction took place with increasing burial, and finally carbonate grains were replaced and cement was precipitated during silica diagenesis, thereby producing chert.

Table 2. X-Ray diffraction mineralogy of Rex Chert, cherty shale, and Meade Peak samples

SAMPLE	LITHOLOGY	MAJOR	MODERATE	MINOR/ TRACE
Section 1				
601-27-1N	Cherty-calcareous shale bed	quartz	feldspar	dolomite, gypsum, smectite(?)
601-27-1M	Laminated siliceous shale	quartz	feldspar	illite, smectite, CFA
601-27-1L2	Siliceous dolostone	quartz	dolomite	calcite, feldspar, smectite(?)
601-27-1L1	Argillaceous chert bed	quartz	feldspar	goethite
601-27-1K2	Argillaceous chert bed	quartz	--	dolomite, feldspar, smectite, gypsum(?)
601-27-1K	Shaly interbed	quartz	--	feldspar, smectite, illite, CFA
601-27-1J	Cherty shale bed	quartz	--	feldspar, illite, CFA, calcite, dolomite
601-27-1I	Phosphatic-ferruginous chert bed	quartz	CFA	clay mineral
601-27-1H	Chert bed	quartz	--	illite, CFA, smectite(?)
601-27-1G	Base of massive thick chert bed	quartz	--	CFA, heulandite(?)
601-27-1F	Chert bed	quartz	--	smectite(?)
601-27-1E	Chert bed	quartz	--	CFA, smectite(?), chlorite or kaolinite(?)
601-27-1D	Chert bed	quartz	--	clay mineral
601-27-1C	Chert bed	quartz	--	dolomite, calcite, smectite(?)
601-27-1B	Chert bed	quartz	--	dolomite, calcite, smectite(?)
601-27-1A	Siliceous limestone bed	calcite	quartz	dolomite, smectite(?)
Section 5				
601-26-1A	Chert bed	quartz	--	--
601-26-1B	Leached zone in chert	quartz	--	kaolinite or chlorite, goethite, bixbyite
601-26-1C	Chert bed	quartz	--	illite, chlorite or kaolinite
601-26-1D	Chert bed	quartz	--	illite, chlorite or kaolinite
Section 7				
601-28-1R1	Breccia	quartz	--	dolomite
601-28-1Q	Chert bed	quartz	--	CFA(?)
502-14-2G	Chert bed	quartz	--	CFA
502-14-2F	Chert bed	quartz	--	CFA, clay minerals
502-14-2E	Chert bed	uartz	--	CFA, clay minerals
601-28-1P	Chert bed	quartz	--	calcite, dolomite, clay minerals
601-28-1N	1N-1K=parts of a 80 cm thick	quartz	--	--
601-28-1M	white chert bed	quartz	--	clay minerals
601-28-1L	chert	quartz	--	smectite(?)
601-28-1K	chert	quartz	--	smectite(?)
601-28-1J3	Chert	quartz	--	CFA(?)
601-28-1J2	Chert	quartz	--	--
601-28-1J1	Chert	quartz	--	smectite(?)
601-28-1I	Chert bed	quartz	--	CFA(?)
601-28-1H	Chert bed	quartz	--	CFA(?), smectite(?)
601-28-1G1	Chert	quartz	--	CFA(?), gypsum
601-28-1G2	Chert	quartz	--	CFA, clay minerals
601-28-1G3	Chert	quartz	--	CFA, smectite
601-28-1F	Phosphatic cherty shale bed	quartz	CFA	illite, smectite(?)
601-28-1E	Siliceous siltstone	quartz	plagioclase	Illite
601-28-1D	Siliceous siltstone, marker bed	quartz	feldspar	illite, smectite(?), jarosite(?)
601-28-1C	Phosphatic-calcareous shale	quartz	CFA, calcite, feldspar	illite, natrojarosite
502-14-2D	Phosphorite	CFA	--	quartz, clay minerals
502-14-2C	Carbonate nodule in black shale	calcite	CFA, dolomite	--
502-14-2B	Phosphatic shale	CFA	calcite, quartz	dolomite, plagioclase, illite
601-28-1B	Carbonate nodule in black shale	calcite	dolomite, CFA	quartz
502-14-2A	Phosphatic shale	CFA, calcite	quartz, plagioclase	pyrite (?), dolomite, mica, clay minerals
601-28-1A	Black phosphatic shale	quartz	feldspar, CFA	calcite, dolomite, illite, pyrite

The cherty shale member from section 1 consists of siliceous siltstone beds and one siliceous dolostone bed. Beds are laminated, contain ghosts of spicules, and some beds contain various combinations of sparse rhombs, bivalves, fish debris, feldspar, fibrous clay minerals, and calcite. Carbonate minerals are more common than they are in the underlying chert. Grains are well sorted. Uncommon sedimentary structures include burrows and reverse grading.

The siliceous siltstone from the Meade Peak-Rex Chert transition zone in section 7 is somewhat different from siliceous siltstone in section 1. The section 7 siltstone is more compacted and shows a preferred fabric created by aggregate extinction of clay minerals, or by parallel orientation of thin wavy iron-rich or organic-matter-rich lenses. Grains are moderately well sorted and range from angular to subrounded, but are predominantly subangular. Similar to section 1, siltstone beds are laminated, contain ghosts of spicules, and some beds contain various combinations of bivalves, fish debris, feldspar, and fibrous clay minerals, as well as mica and chlorite; however no rhombs or calcite were seen.

Mineralogy

The mineral content of the Rex Chert and cherty shale member is dominated by quartz (Table 2). Several beds also have major amounts of carbonate minerals: the lowermost bed in section 1 (601-27-1A), which contains major calcite as well as quartz; and a siliceous dolostone (601-27-1L2) in section 1 contains major dolomite as well as quartz. Feldspar (combined K-feldspar and plagioclase), dolomite, and carbonate fluorapatite (CFA) occur in moderate amounts in a few beds (Table 2). Clay minerals occur in minor amounts. In the upper part of the Meade Peak Member in section 7, calcite and CFA are major phases along with quartz in some samples.

Chemical Composition

The mean concentrations of elements in the Rex Chert and the cherty shale member are overwhelmingly dominated by silica, which averages 94.6% for the three sections studied and ranges from 92.2% for section 1 to 96.9% for section 5 (Table 3). The sums of the major oxides are reasonable close to 100%, but are a little high for most of the stratigraphically highest 13 samples from section 7, up to 103% (Table 3). These high values provide a measure of the analytical accuracy of silica determinations for these very high silica rocks. Samples with low sums of the major oxides results from not including organic carbon and sulfur compounds in those totals, which occur predominantly for the Meade Peak rocks in section 7.

Organic carbon contents are generally very low in the chert, but are up to 1.8% in samples from the cherty shale member in section 1 and up to 3.4% in rocks from the transition between the Meade Peak and Rex Chert in section 7 (Table 3). Likewise, phosphate (P_2O_5) is generally very low in the chert, but can be high (up to 3.1%) in individual beds; these beds do not consistently occur at any particular stratigraphic level in the sections.

Selenium concentrations for the Rex Chert and cherty shale member vary from the detection limit (<0.2) to 138 ppm, with a mean concentration of 7 ppm (Table 4), or <1.0 ppm if two outliers are removed.

Mean Se concentrations vary from 0.65 ppm in section 5 (Tables 6) to 12 ppm for section 7 (Table 7; this does not include values from Meade Peak rocks). The mean Se concentration for section 5 rocks is equivalent to that of mean shale, 0.6 ppm (Krauskopf, 1979), whereas that of section 1 (Table 5) is 2.2 times the concentration in mean shale and section 7 is 20 times the mean shale concentration. The reason for these differences is that section 7 includes the lowermost Rex Chert, which contains rocks of transitional character, and section 1 includes the cherty shale member. All the chert beds in the upper part of the Rex Chert in section 7 have Se concentrations of <0.2 to 0.8 ppm and the mean concentration of

Table 4. Statistics for 39 Rex Chert and cherty shale samples collected from measured sections 1, 5, and 7

		N	Mean	Median	SD[1]	Minimum	Maximum
SiO_2	wt%	39	94.6	96.3	6.79	74.9	102
Al_2O_3		39	1.82	0.72	2.64	0.23	11.1
Fe_2O_3		39	0.70	0.31	0.96	0.04	4.68
TiO_2		39	0.11	0.03	0.19	0.01	0.82
CaO		39	0.88	0.46	0.86	0.17	3.69
K_2O		39	0.35	0.10	0.63	0.005	2.58
MgO		39	0.25	0.08	0.32	0.01	1.09
Na_2O		39	0.19	0.05	0.31	0.01	1.32
P_2O_5		39	0.42	0.25	0.54	0.05	3.05
$\sum CO_2$		39	0.31	0.02	0.67	0.005	2.78
Total		39	99.7	99.9	2.51	93.1	103
C_t		39	0.42	0.17	0.65	0.01	3.35
C_c		39	0.09	0.01	0.18	0.0015	0.76
C_{org}		39	0.33	0.12	0.61	0.007	3.347
S_t		39	0.05	0.025	0.07	0.025	0.42
As	ppm	39	4.22	2.50	4.45	0.30	16.8
Ba		39	112	50	143	17	593
Ba		39	111	49	140	16	611
Ce		39	11	3	17	2.5	87
Cr		39	143	67	227	5	1100
Cu		39	46	31	58	5	296
Hg		39	0.04	0.03	0.04	0.01	0.16
La		39	16	9	28	3	176
Li		39	10	8	8	1	43
Mn		39	128	55	272	13	1710
Nd		39	17	5	31	4.5	197
Ni		39	25	16	23	4	98
Sb		39	0.9	0.3	1.8	0.3	11.4
Se		39	7.1	0.8	26.8	0.1	138
Sr		39	39	24	37	8	215
V		39	30	15	40	1	188
Y		39	26	13	51	2	321
Zn		39	110	90	107	24	569
Zr		39	48	16	89	5	397

[1]Standard Deviation

Table 5. Statistics for 14 Rex Chert and cherty shale samples collected from measured sections 1

		N	Mean	Median	SD[1]	Minimum	Maximum
SiO_2	wt %	14	92.2	93.1	6.28	78.7	99.9
Al_2O_3		14	2.23	1.80	2.18	0.26	8.41
Fe_2O_3		14	1.17	0.77	1.24	0.17	4.68
TiO_2		14	0.13	0.08	0.15	0.01	0.55
CaO		14	1.32	1.05	0.96	0.21	3.69
K_2O		14	0.43	0.26	0.51	0.02	1.95
MgO		14	0.42	0.25	0.39	0.01	1.09
Na_2O		14	0.24	0.07	0.25	0.01	0.63
P_2O_5		14	0.62	0.41	0.74	0.09	3.05
$\sum CO_2$		14	0.56	0.06	0.77	0.01	2.15
Total		14	99.3	99.6	1.5	95.4	101
C_t		14	0.63	0.39	0.58	0.01	1.81
C_c		14	0.15	0.02	0.21	0.0015	0.59
C_{org}		14	0.48	0.31	0.50	0.007	1.8
S_t		14	0.05	0.03	0.05	0.025	0.2
As	ppm	14	4.3	3.1	4.0	0.7	13.2
Ba		14	142	68	179	18	593
Ba		14	140	70	177	16	611
Ce		14	17	11	22	2.5	87
Cr		14	239	138	310	19	1100
Cu		14	38	31	35	11	152
Hg		14	0.05	0.04	0.04	0.01	0.15
La		14	25	15	44	3	176
Li		14	14	11	11	4	43
Mn		14	68	46	80	13	333
Nd		14	31	22	49	4.5	197
Ni		14	29	21	24	4	97
Sb		14	0.6	0.3	0.5	0.3	2.2
Se		14	1.3	1.1	0.8	0.1	2.8
Sr		14	54	39	51	14	215
V		14	39	26	47	4	188
Y		14	48	31	80	6	321
Zn		14	88	90	38	30	154
Zr		14	51	30	49	5	164

[1]Standard Deviation

Table 6. Statistics for 4 Rex Chert and cherty shale samples collected from measured sections 5

		N	Mean	Median	SD[1]	Minimum	Maximum
SiO_2	wt %	4	96.9	97.5	2.05	93.9	98.6
Al_2O_3		4	1.05	1.07	0.39	0.55	1.49
Fe_2O_3		4	0.98	0.48	1.12	0.31	2.65
TiO_2		4	0.05	0.04	0.03	0.017	0.08
CaO		4	0.30	0.27	0.09	0.22	0.43
K_2O		4	0.15	0.17	0.05	0.07	0.18
MgO		4	0.09	0.09	0.03	0.05	0.12
Na_2O		4	0.05	0.05	0.01	0.04	0.07
P_2O_5		4	0.19	0.16	0.08	0.14	0.3
$\sum CO_2$		4	0.02	0.02	0.01	0.01	0.03
Total		4	100	100	0.37	99.2	100
C_t		4	0.13	0.12	0.04	0.09	0.19
C_c		4	0.01	0.01	0.00	0.0015	0.01
C_{org}		4	0.12	0.11	0.05	0.08	0.187
S_t		4	0.03	0.03	0.01	0.025	0.05
As	ppm	4	5.3	2.6	6.2	1.6	14.5
Ba		4	227	200	154	85	423
Ba		4	219	188	152	84	415
Ce		4	5	6	2	2.5	8
Cr		4	70	73	13	51	81
Cu		4	32	28	20	13	60
Hg		4	0.05	0.03	0.04	0.02	0.1
La		4	6	6	3	4	10
Li		4	10	10	3	6	13
Mn		4	449	33	841	22	1710
Nd		4	10	10	4	4.5	15
Ni		4	33	12	44	8	98
Sb		4	0.8	0.8	0.2	0.7	1.0
Se		4	0.7	0.6	0.2	0.5	0.9
Sr		4	30	24	14	22	51
V		4	20	17	11	11	35
Y		4	14	13	4	10	20
Zn		4	92	48	102	29	244
Zr		4	25	25	16	5	45

[1]Standard Deviation

Table 7. Statistics for 21 Rex Chert and cherty shale samples collected from measured sections 7

		N	Mean	Median	SD[1]	Minimum	Maximum
SiO_2	wt %	21	95.9	96.7	7.38	74.9	102
Al_2O_3		21	1.69	0.43	3.15	0.23	11.1
Fe_2O_3		21	0.34	0.14	0.51	0.04	2.09
TiO_2		21	0.11	0.02	0.23	0.01	0.82
CaO		21	0.70	0.41	0.74	0.17	2.92
K_2O		21	0.34	0.05	0.76	0.005	2.58
MgO		21	0.16	0.03	0.24	0.01	0.7
Na_2O		21	0.18	0.07	0.36	0.03	1.32
P_2O_5		21	0.33	0.23	0.39	0.05	1.72
$\sum CO_2$		21	0.21	0.02	0.64	0.005	2.78
Total		21	99.9	101	3.2	93.1	103
C_t		21	0.34	0.12	0.73	0.01	3.35
C_c		21	0.06	0.01	0.17	0.0015	0.76
C_{org}		21	0.28	0.08	0.72	0.007	3.347
S_t		21	0.05	0.03	0.09	0.025	0.42
As	ppm	21	4.0	2.2	4.6	0.3	16.8
Ba		21	70	37	97	17	365
Ba		21	70	39	93	22	351
Ce		21	8	3	13	2.5	47
Cr		21	93	16	158	5	601
Cu		21	54	33	73	5	296
Hg		21	0.03	0.01	0.04	0.01	0.16
La		21	12	6	12	3	48
Li		21	8	6	6	1	21
Mn		21	107	58	85	21	299
Nd		21	9	5	9	4.5	37
Ni		21	20	15	19	4	86
Sb		21	1.1	0.3	2.4	0.3	11.4
Se		21	12.1	0.2	36.2	0.1	138
Sr		21	30	19	26	8	95
V		21	25	5	39	1	130
Y		21	14	8	17	3	76
Zn		21	128	91	136	24	569
Zr		21	51	13	115	5	397

[1]Standard Deviation

12 ppm is heavily dependent on two sample values of 101 and 138 ppm. Without those two samples, the mean Se concentration in section 7 would be 0.8 ppm Se, close to its crustal mean content (Table 3).

Other elements of environmental interest include As, Cr, V, Zn, Hg, and Cd. Arsenic concentrations vary by a factor of 56, from 0.3 to 16.8 ppm, mean 4.2 ppm, which is slightly less than the concentration in average shale of 6.6 ppm (Govett, 1983). Chromium concentrations vary by a factor of 220, from 5 to 1100 ppm, with a mean of 143 ppm, which is higher than the 100 ppm concentration in average shale. Vanadium concentrations vary by a factor of 188, from 1 to 188 ppm, mean 30 ppm, which is much lower than the 130 ppm concentration in average shale. Zinc concentrations vary by a factor of 24, from 24 to 569 ppm, mean 110 ppm, which is somewhat greater than the concentration in average shale of 80 ppm. Mercury concentrations vary by a factor of >8, from 0.01 to 0.16 ppm, mean 0.04 ppm, which is an order of magnitude less than the concentration in average shale of 0.4 ppm. Cadmium concentrations are uniformly below the limit of quantification (<2 ppm) except for rocks from the lowermost part of section 7; we are unable to ascertain whether the average may be higher than that of average shale, 0.3 ppm.

Stratigraphic Changes in Chemical Composition

Stratigraphic changes (equivalent to temporal changes in the depositional basin) in chemical composition of rocks are notable either as uniform changes through the sections or as distinct differences in the mean composition of rocks that compose the upper and lower halves of the sections. In this regard, most elements increase up section in section 1, whereas they decrease up section in sections 5 and 7. These increases up section in section 1 still occur for about half of the elements if the cherty shale member is not included in the analysis; the other half of the elements do not vary uniformly up section. Silica has the opposite trend of the other elements. For section 1 (including the cherty shale member), the following elements increase up section: Al, Fe, Ti, K, Na, As, Ba, Ce, Cr, Hg, La, Li, Ni, Sc, Sr, V, and Zr; in contrast, silica decreases up section and Ca, Mg, C, and Mn decrease to near mid-section then increase farther up section. For section 5, the following elements decrease up section: Al, Fe, Ti, K, Na, C, Ce, Ni, Sr, V, Y, and Zn; whereas Si increases up section. For section 7, the following elements decrease up section: Al, Fe, Ti, K, Na, organic C, Ba, Ce, Cr, La, Li, Ni, Se, Sr, Tl, V, Y, Zn, and Zr; whereas Si and Mn increase up section.

Phase Associations of Elements

The phase associations of elements were determined by comparing results from element correlations determined from correlation coefficient matrices (Tables 8-10), rotated factor loadings from Q-mode factor analyses (Figures 3-5), and mineralogy as determined by XRD (Table 2). Three data sets were analyzed including data from sections 1, 5, and 7 combined, section 1 data, and section 7 data (excluding Meade Peak and Rex Chert carbonate beds).

We consider four to five Q-mode factors that are interpreted to represent the following rock and mineral components: **Factor 1**, Chert-silica component consisting solely of Si, except for the combined data set where Ba shows a minor but statistically significant factor loading. **Factor 2**, phosphorite-phosphate component comprised of P, Ca, As, Y, V, Cr, Sr, and La (± Fe, Zn, Cu, Ni, Li, Se, Nd, and Hg depending on the data set). **Factor 3**, shale component comprised of Al, Na, Zr, K, Ba, Li, and organic C (± Ti, Mg, Se, Ni, Fe, Sr, V, Mn, and Zn depending on the data set). **Factor 4**, carbonate component (dolomite, calcite, silicified carbonates) comprised of carbonate C, Mg, Ca, and Si (± Mn). **Factor 5** we tentatively interpret as representing organic matter (and/or sulfide-sulfate phases) hosted elements comprised of Cu (± organic C, Zn, Mn Si, Ni, Hg, and Li depending on the data set). Copper correlates only with Zn, but Zn also correlates with Ni, As and some elements associated with the shale component. Silica is dominantly in the

Table 8. Correlation coefficient matrix for 39 samples from sections 1, 5, and 7 combined listed in Table 3; the point of zero correlation for n=39 at the 99% confidence level is |0.4047|

	SiO_2	Al_2O_3	Fe_2O_3	TiO_2	CaO	K_2O	MgO	Na_2O	P_2O_5	$\sum CO_2$	C_T	C_C	C_{org}	As	Ba	Cr	Cu	La	Li	Mn
Al_2O_3	-0.900																			
Fe_2O_3	-0.714	0.553																		
TiO_2	-0.878	0.995	0.496																	
CaO	-0.371	0.065	0.471	0.022																
K_2O	-0.893	0.995	0.553	0.992	0.062															
MgO	-0.674	0.556	0.382	0.550	0.626	0.544														
Na_2O	-0.824	0.939	0.419	0.953	-0.003	0.916	0.570													
P_2O_5	-0.349	0.092	0.737	0.021	0.682	0.099	0.111	-0.080												
$\sum CO_2$	-0.113	-0.045	-0.103	-0.031	0.647	-0.054	0.742	0.045	-0.108											
C_T	-0.782	0.763	0.415	0.768	0.223	0.772	0.739	0.737	-0.042	0.342										
C_C	-0.111	-0.048	-0.105	-0.034	0.645	-0.058	0.739	0.042	-0.110	1.000	0.340									
C_{org}	-0.797	0.824	0.472	0.825	0.044	0.836	0.564	0.769	-0.011	0.065	0.960	0.063								
As	-0.610	0.516	0.697	0.457	0.382	0.522	0.240	0.315	0.670	-0.196	0.415	-0.199	0.501							
Ba	-0.544	0.565	0.247	0.570	0.094	0.547	0.553	0.612	-0.062	0.170	0.517	0.166	0.499	0.164						
Cr	-0.717	0.537	0.926	0.472	0.565	0.547	0.404	0.331	0.813	-0.076	0.425	-0.080	0.475	0.826	0.230					
Cu	0.032	0.030	-0.007	0.016	0.016	0.030	-0.115	-0.013	0.147	-0.164	-0.044	-0.168	0.003	0.255	-0.097	0.095				
La	-0.501	0.277	0.849	0.225	0.618	0.298	0.221	0.130	0.909	-0.092	0.130	-0.095	0.166	0.620	0.081	0.864	0.061			
Li	-0.705	0.587	0.913	0.535	0.426	0.565	0.386	0.500	0.660	-0.106	0.368	-0.110	0.423	0.668	0.356	0.854	0.118	0.770		
Mn	0.274	-0.182	-0.126	-0.163	-0.157	-0.214	-0.113	-0.051	-0.222	0.030	-0.183	0.030	-0.204	-0.253	-0.233	-0.225	0.028	-0.211	-0.008	
Ni	-0.626	0.572	0.497	0.518	0.361	0.534	0.448	0.442	0.377	0.046	0.448	0.043	0.463	0.675	0.295	0.645	0.242	0.267	0.585	0.052
Se	-0.643	0.806	0.262	0.838	-0.160	0.827	0.290	0.815	-0.131	-0.108	0.664	-0.110	0.737	0.304	0.402	0.197	-0.007	0.111	0.271	-0.176
Sr	-0.717	0.502	0.846	0.453	0.669	0.508	0.476	0.382	0.823	0.051	0.371	0.046	0.380	0.671	0.409	0.883	0.050	0.916	0.816	-0.315
V	-0.756	0.612	0.872	0.557	0.526	0.623	0.356	0.433	0.796	-0.126	0.442	-0.130	0.509	0.874	0.259	0.940	0.165	0.855	0.832	-0.284
Y	-0.384	0.127	0.822	0.068	0.647	0.144	0.169	-0.018	0.938	-0.070	0.019	-0.073	0.043	0.550	0.011	0.823	0.041	0.977	0.719	-0.193
Zn	-0.195	0.187	0.132	0.141	0.292	0.162	0.029	0.072	0.415	-0.101	0.004	-0.104	0.035	0.609	-0.031	0.347	0.620	0.176	0.253	-0.014
Zr	-0.823	0.963	0.420	0.980	-0.039	0.963	0.500	0.958	-0.050	-0.035	0.746	-0.038	0.803	0.369	0.557	0.365	-0.007	0.180	0.463	-0.157

	Ni	Se	Sr	V	Y	Zn
Se	0.101					
Sr	0.434	0.271				
V	0.581	0.411	0.902			
Y	0.221	-0.062	0.868	0.778		
Zn	0.665	0.012	0.251	0.457	0.143	
Zr	0.369	0.915	0.403	0.495	0.015	0.069

Table 9. Correlation coefficient matrix for 14 samples from section 1 listed in Table 3; the point of zero correlation for n=14 at the 99% confidence level is |0.651|

	SiO_2	Al_2O_3	Fe_2O_3	TiO_2	CaO	K_2O	MgO	Na_2O	P_2O_5	ΣCO_2	C_T	C c	C_{org}	As	Ba	Ce	Cr	Cu	Hg	La	Li	Mn
Al_2O_3	-0.884																					
Fe_2O_3	-0.717	0.514																				
TiO_2	-0.858	0.993	0.436																			
CaO	-0.573	0.136	0.523	0.105																		
K_2O	-0.895	0.984	0.549	0.968	0.190																	
MgO	-0.697	0.548	0.132	0.580	0.608	0.535																
Na_2O	-0.666	0.784	0.234	0.814	0.055	0.672	0.592															
P_2O_5	-0.476	0.134	0.851	0.050	0.704	0.212	0.012	-0.148														
ΣCO_2	-0.181	-0.004	-0.322	0.053	0.502	-0.027	0.806	0.233	-0.257													
C_T	-0.754	0.774	0.101	0.800	0.322	0.776	0.863	0.669	-0.114	0.551												
C c	-0.175	-0.008	-0.326	0.048	0.498	-0.032	0.803	0.229	-0.261	1.000	0.547											
C_{org}	-0.805	0.906	0.254	0.912	0.167	0.918	0.670	0.683	-0.023	0.224	0.937	0.220										
As	-0.738	0.644	0.907	0.566	0.383	0.707	0.151	0.220	0.732	-0.377	0.236	-0.379	0.434									
Ba	-0.432	0.436	0.002	0.482	0.247	0.395	0.654	0.605	-0.103	0.429	0.547	0.422	0.461	0.076								
Ce	-0.737	0.458	0.940	0.393	0.695	0.516	0.260	0.180	0.894	-0.151	0.186	-0.157	0.282	0.850	0.128							
Cr	-0.812	0.610	0.944	0.541	0.589	0.681	0.273	0.221	0.827	-0.216	0.307	-0.222	0.451	0.927	0.089	0.961						
Cu	0.007	0.055	-0.051	0.052	-0.215	0.090	-0.107	-0.059	-0.117	-0.164	0.122	-0.166	0.212	-0.036	-0.070	-0.026	0.058					
Hg	-0.802	0.700	0.855	0.638	0.415	0.763	0.243	0.295	0.699	-0.309	0.357	-0.313	0.547	0.912	0.198	0.817	0.919	0.163				
La	-0.512	0.167	0.869	0.094	0.717	0.244	0.074	-0.097	0.967	-0.204	-0.069	-0.209	0.008	0.741	-0.043	0.946	0.866	-0.061	0.700			
Li	-0.722	0.560	0.928	0.511	0.446	0.550	0.204	0.429	0.702	-0.252	0.140	-0.258	0.271	0.795	0.188	0.870	0.854	-0.001	0.809	0.766		
Mn	-0.188	0.274	0.176	0.291	-0.163	0.121	0.086	0.648	-0.167	-0.010	0.031	-0.008	0.039	-0.023	0.067	-0.026	-0.038	-0.100	0.022	-0.137	0.415	
Nd	-0.517	0.178	0.883	0.101	0.708	0.254	0.063	-0.091	0.976	-0.226	-0.074	-0.231	0.011	0.756	-0.037	0.949	0.871	-0.066	0.709	0.997	0.768	-0.142
Ni	-0.797	0.968	0.411	0.967	-0.008	0.930	0.471	0.807	0.009	-0.050	0.739	-0.052	0.883	0.536	0.382	0.312	0.486	0.149	0.641	0.027	0.502	0.402
Se	-0.513	0.329	0.325	0.310	0.527	0.302	0.449	0.462	0.407	0.209	0.377	0.201	0.356	0.249	0.580	0.451	0.355	-0.087	0.311	0.369	0.355	0.025
Sr	-0.677	0.318	0.823	0.264	0.843	0.378	0.355	0.120	0.904	0.035	0.188	0.028	0.207	0.706	0.251	0.950	0.862	-0.091	0.715	0.939	0.766	-0.118
V	-0.698	0.421	0.955	0.343	0.663	0.493	0.181	0.082	0.927	-0.229	0.129	-0.234	0.249	0.883	0.025	0.982	0.969	0.030	0.858	0.952	0.850	-0.064
Y	-0.483	0.132	0.867	0.054	0.714	0.209	0.039	-0.131	0.984	-0.225	-0.108	-0.229	-0.029	0.731	-0.073	0.930	0.848	-0.065	0.686	0.994	0.744	-0.150
Zn	-0.393	0.546	0.148	0.526	-0.176	0.510	0.214	0.484	-0.136	-0.070	0.455	-0.067	0.559	0.207	0.108	-0.020	0.143	0.502	0.337	-0.213	0.135	0.298
Zr	-0.843	0.959	0.384	0.976	0.145	0.908	0.627	0.890	0.023	0.140	0.801	0.134	0.878	0.469	0.569	0.363	0.470	-0.004	0.547	0.061	0.491	0.355

	Nd	Ni	Se	Sr	V	Y	Zn
Ni	0.034						
Se	0.391	0.262					
Sr	0.940	0.165	0.592				
V	0.958	0.292	0.378	0.920			
Y	0.998	-0.006	0.382	0.929	0.947		
Zn	-0.175	0.635	0.106	-0.137	0.047	-0.177	
Zr	0.071	0.933	0.438	0.274	0.287	0.025	0.501

Table 10. Correlation coefficient matrix for 21 samples from section 7 listed in Table 3; the point of zero correlation for n=21 at the 99% confidence level is |0.542|

	SiO_2	Al_2O_3	Fe_2O_3	CaO	K_2O	MgO	Na_2O	P_2O_5	ΣCO_2	C_T	C_{org}	As	Ba	Cr	Cu	La	Li	Mn
Al_2O_3	-0.924																	
Fe_2O_3	-0.877	0.867																
CaO	-0.097	-0.061	0.119															
K_2O	-0.918	0.999	0.864	-0.079														
MgO	-0.646	0.654	0.564	0.485	0.661													
Na_2O	-0.896	0.987	0.793	-0.151	0.990	0.645												
P_2O_5	-0.141	0.004	0.331	0.580	-0.030	-0.056	-0.146											
ΣCO_2	0.062	-0.136	-0.164	0.718	-0.127	0.623	-0.121	-0.140										
C_T	-0.770	0.758	0.813	0.017	0.776	0.689	0.757	-0.158	0.141									
C_{org}	-0.789	0.795	0.857	-0.154	0.811	0.544	0.790	-0.124	-0.098	0.971								
As	-0.558	0.461	0.787	0.390	0.447	0.325	0.336	0.735	-0.139	0.486	0.523							
Ba	-0.927	0.995	0.844	-0.107	0.995	0.629	0.989	-0.037	-0.160	0.746	0.788	0.419						
Cr	-0.685	0.600	0.880	0.402	0.584	0.404	0.469	0.721	-0.137	0.529	0.565	0.930	0.562					
Cu	0.018	0.027	0.148	0.148	0.016	-0.109	-0.007	0.410	-0.170	-0.072	-0.030	0.338	0.000	0.230				
La	-0.710	0.637	0.819	0.409	0.611	0.373	0.514	0.765	-0.187	0.386	0.434	0.855	0.605	0.945	0.347			
Li	-0.770	0.778	0.856	0.218	0.762	0.477	0.698	0.480	-0.178	0.570	0.616	0.726	0.753	0.813	0.347	0.869		
Mn	0.508	-0.393	-0.406	-0.133	-0.379	-0.225	-0.365	-0.302	0.120	-0.277	-0.307	-0.426	-0.362	-0.416	-0.009	-0.473	-0.332	
Ni	-0.477	0.363	0.631	0.620	0.337	0.294	0.221	0.862	-0.003	0.209	0.211	0.800	0.332	0.883	0.344	0.899	0.709	-0.200
Sr	-0.852	0.789	0.884	0.337	0.768	0.520	0.692	0.601	-0.144	0.532	0.570	0.815	0.766	0.908	0.245	0.964	0.895	-0.530
V	-0.796	0.737	0.936	0.331	0.722	0.483	0.625	0.627	-0.156	0.609	0.650	0.897	0.705	0.977	0.261	0.958	0.890	-0.461
Y	-0.277	0.141	0.447	0.580	0.107	0.048	-0.008	0.984	-0.136	-0.047	-0.014	0.766	0.103	0.796	0.414	0.848	0.583	-0.337
Zn	-0.228	0.157	0.441	0.569	0.127	0.071	0.018	0.933	-0.109	-0.043	-0.016	0.739	0.115	0.752	0.622	0.820	0.607	-0.179
Zr	-0.891	0.988	0.814	-0.155	0.992	0.651	0.996	-0.145	-0.121	0.781	0.814	0.354	0.988	0.490	-0.021	0.518	0.707	-0.339

	Ni	Sr	V	Y	Zn
Sr	0.810				
V	0.836	0.963			
Y	0.916	0.705	0.722		
Zn	0.910	0.671	0.696	0.951	
Zr	0.225	0.689	0.639	-0.008	0.018

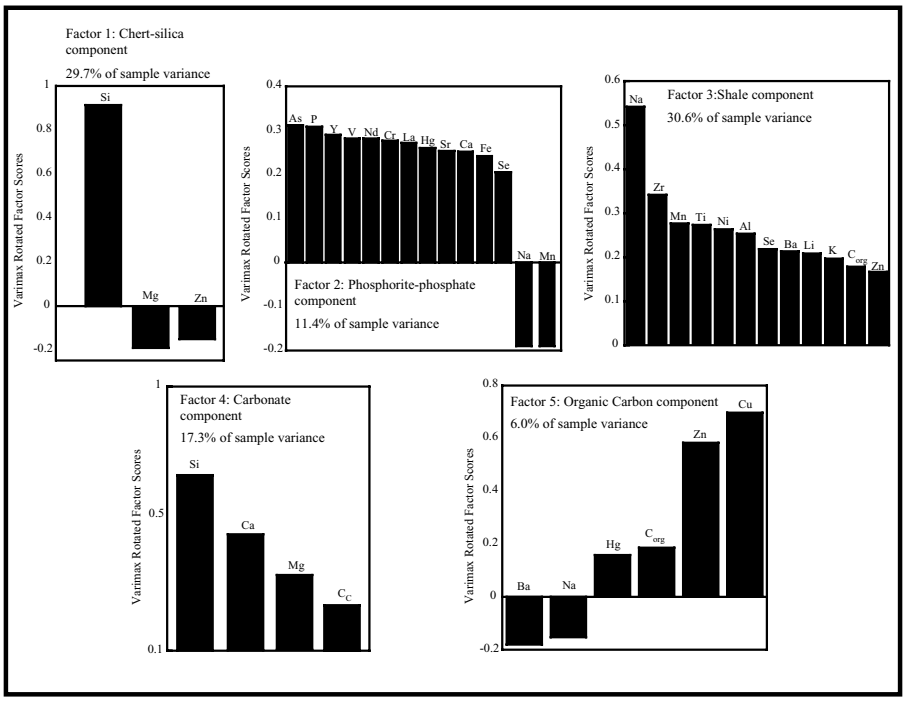

Figure 3. Q-mode factors for Rex Chert and cherty shale samples from sections 1, 5, and 7

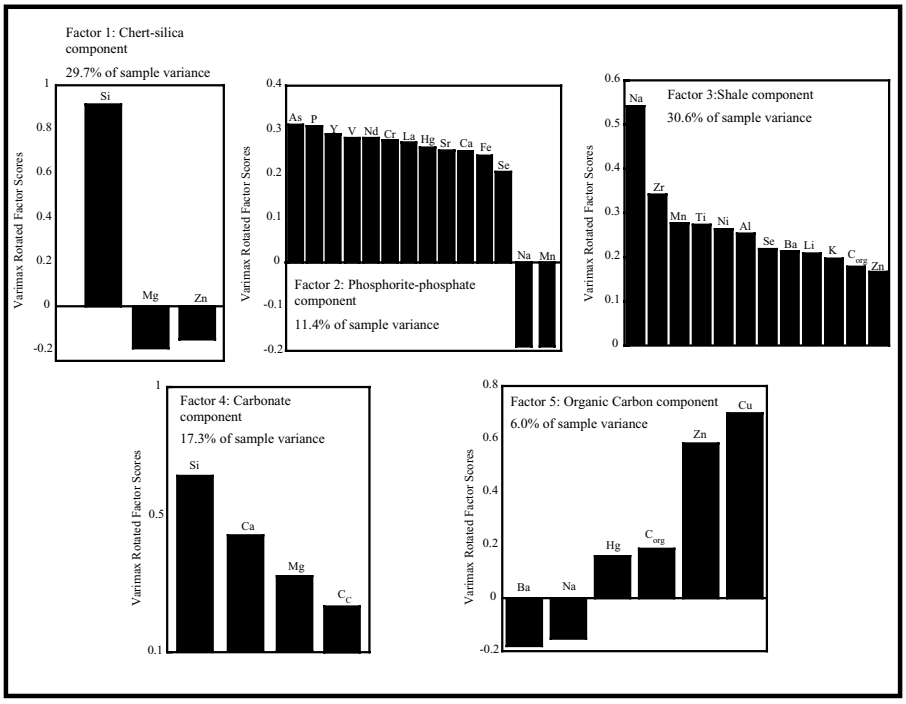

Figure 4. Q-mode factors for Rex Chert and cherty shale samples from section 1

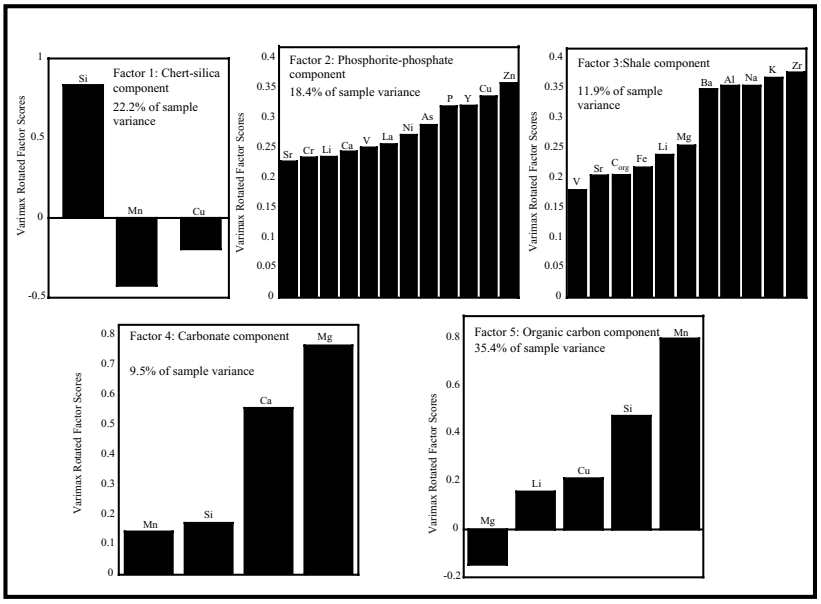

Figure 5. Q-mode factors for Rex Chert and cherty shale samples from section 7

chert fraction (factor 1) and does not show up in the aluminosilicate fraction (factor 3 shale fraction) even though it is clearly part of the feldspars and clay minerals that comprise that fraction. Likewise, organic C is dominantly in Factor 3 and does not show up in factor 5 (except for section 1) even though it is likely that the elements in factor 5 are hosted by organic matter. These characteristics are an artifact of analyzing a data set that is overwhelmingly dominated by one variable, silica, and the distribution of some elements in more than one phase. Selenium shows a dominant association with the shale component, but correlations and Q-mode factors also indicate that organic matter (within the shale component) and carbonate fluorapatite may host a portion of the Se. Consideration of larger numbers of factors in Q-mode analysis indicates that native Se (a factor containing Se ± Ba) may also comprise a minor component of the Se compliment.

DISCUSSION AND CONCLUSIONS

The chert beds generally have Se concentrations of <1 ppm. The cherty shale member rocks have a somewhat higher Se contents, mean 1.8 ppm. Siliceous siltstone and argillaceous chert that comprise the zone of transition between the Meade Peak and Rex Chert have Se concentrations up to 138 ppm.

The low Se contents determined for the chert-bed samples here are not characteristic of Se concentrations found for composite channel samples of chert at the Rasmussen Ridge and Enoch Valley Mines (Herring et al., 2002). Those weighted (for stratigraphic thickness) mean Se concentrations are 63 ppm for the Rasmussen Ridge samples and 18 ppm for the Enoch Valley samples. These differences may result from several factors, such as weathering of the outcrop samples we analyzed and the inclusion of shale and siliceous shale beds that are interbedded with cherts in the composite samples. This latter influence is supported by the lower silica and higher Al_2O_3, K_2O, etc. contents of the composite samples. In the outcrop sections studied here, shale interbedded with the chert consists only of thin partings, except in the cherty shale member, and those partings would

not likely contribute significantly to the mean Se concentration for each outcrop section. It is not known why there are more (or thicker) shale interbeds, or more argillaceous cherts in the composite sections than those studied in outcrops. Chert is very resistant to weathering and little Se should be leached by weathering of the outcrops.

Other elements of environmental interest include As, Cr, V, Zn, Hg, and Cd. Of these elements, only mean Cr and Zn values are higher than their respective values in average shale, 30% and 27% higher, respectively. Cadmium could not be evaluated because most concentrations are below the limit of quantification of 2 ppm.

ACKNOWLEDGMENTS

We thank Dick Grauch for reviewing this report.

REFERENCES CITED

Arbogast, B.F., (ed.), 1996, Analytical methods manual for the Mineral Resource Surveys Program, U.S. Geological Survey: U.S. Geological Survey Open-File Report 96-525, 248 p.

Baedecker, P.A., (ed.), 1987, Methods for geochemical analysis: U.S. Geological Survey Bulletin 1770, variously paginated.

Brittenham, M.D., 1976, Permian Phosphoria carbonate banks, Idaho-Wyoming thrust belt, *in* Hill, J.G., ed., Symposium on geology of the Cordilleran hingeline: Rock Mountain Association of Geologists—1976 symposium, Denver, p. 173-191.

Cressman, E.R., and Swanson, R.W., 1964, Stratigraphy and petrology of the Permian rocks of southwestern Montana: U.S. Geological Survey Professional Paper 313-C, p. 275-569.

Govett, G.J.S., 1983, Handbook of Exploration Geochemistry, v. 3, Rock Geochemistry in Mineral Exploration. Elsevier, Amsterdam, 461 pp.

Herring, J.H., et. al. 2002, in preparation

Gulbrandsen, R.A., 1966, Chemical composition of phosphorites of the Phosphoria Formation: Geochimica et Cosmochimica Acta, v. 30, p. 769-778.

Gulbrandsen, R.A., 1975, Analytical data on the Phosphoria Formation, western United States: U.S. Geological Survey Open-File Report 75-554, 45 p.

Gulbrandsen, R.A., 1979, Preliminary analytical data on the Meade Peak member of the Phosphoria Formation at Hot Springs underground mine, Trail Canyon trench, and Conda underground mine, southeastern Idaho: U.S. Geological Survey Open-File Report 79-369, 35 p.

Gulbrandsen, R.A., and Krier, D.J., 1980, Large and rich phosphorus resources in the Phosphoria Formation in the Soda Springs area southeastern Idaho: U.S. Geological Survey Bulletin 1496, 25 p.

Jackson, L.L., Brown, F.W., and Neil, S.T., 1987, Major and minor elements requiring individual determinations, classical whole rock analysis, and rapid rock analysis, p. G1-G23, *in* Baedecker, P.A., (ed.), Methods for geochemical analysis: U.S. Geological Survey Bulletin 1770.

Klovan J.E. and Imbrie J., 1971, An algorithm and FORTRAN-IV program for large-scale Q-mode factor analysis and calculation of factor scores. Mathematical Geology v. 3, p. 61-77.

Krauskopf, K.B., 1979, Introduction to Geochemistry. McGraw-Hill, New York, 617 pp.
Lee, W.H., 2001, A history of phosphate mining in Southeastern Idaho. U.S. Geological Survey Open-File Report 00-425, Version 1.0, CD-ROM, 253 pp.
McKelvey, V.E., Williams, J.S., Sheldon, R.P., Cressman, E.R., Cheney, T.M., and Swanson, R.W., 1959, The Phosphoria, Park City, and Shedhorn Formations in the Western Phosphate Field: U.S. Geological Survey Professional Paper 313-A, 47 p.
Montgomery, K.M, and Cheney, T.M., 1967, Geology of the Stewart Flat quadrangle, Caribou County, Idaho: U.S. Geological Bulletin 1217, 63 p.
Oberlindacher, H.P., 1990, Geologic map and phosphate resources of the northeastern part of the Lower Valley quadrangle, Caribou County, Idaho: U.S. Geological Survey Miscellaneous Field Studies Map MF-2133, scale 1:12,000.
Service, A.L., 1966, An evaluation of the western phosphate industry and its resources, Part 3. Idaho: U.S. Bureau of Mines Report of Investigations 6801, 201 p.